Article

Discovery Medicine 2026; 38(207): 1103–1114
https://doi.org/10.24976/Discov.Med.202638207.89

HDAC2-STAT1 Axis Mediates the Protective Effect of Acetate in DNCB-Induced Atopic Dermatitis

Xiaoyan He[1,*], Xin Li[1], Haiyan Feng[1]

[1]Department of Dermatology, Peking University First Hospital Taiyuan (Taiyuan Central Hospital), 033000 Taiyuan, Shanxi, China
*Correspondence: hexiaoyan_Hxx@163.com (Xiaoyan He)
Submitted: 14 November 2025 Revised: 28 January 2026 Accepted: 26 February 2026 Published: 20 April 2026

Background: Atopic dermatitis (AD), a persistent inflammatory condition of the skin, presents features of pruritus, skin barrier dysfunction, and immune dysregulation, affecting millions globally with increasing prevalence. Acetate (Ace), a short-chain fatty acid with immunomodulatory and barrier-protective properties, has been reported to enhance skin barrier integrity in AD, but its precise molecular mechanisms remain unclear. This study aims to investigate the therapeutic potential of Ace and its underlying mechanism in an AD mouse model.

Methods: An AD mouse model was established via repeated topical application of 2,4-dinitrochlorobenzene (DNCB) and treated with Ace sodium. Macroscopic situation, AD severity, and dorsal tissue pathology were evaluated. Skin mRNA expression levels of inflammatory factors, histone deacetylase 2 (HDAC2), and signal transducer and activator of transcription 1 (STAT1), as well as HDAC2-STAT1 promoter correlation, were examined using chromatin immunoprecipitation. $CD4^+$ T cells from healthy mouse splenocytes were transfected with HDAC2/STAT1 overexpression plasmids, and treated under Th17-inducing conditions with Ace. Th17/regulatory T (Treg) in splenocytes was assessed by flow cytometry.

Results: Ace mitigated DNCB-induced dryness, erosion of dorsal skin, and ear redness. Furthermore, Ace downregulated the expression levels of pro-inflammatory factors and HDAC2 in the dorsal skin tissue, reduced the proportion of Th17 cells in the splenocytes, and promoted the expression of STAT1. Chromatin immunoprecipitation confirmed the binding of HDAC2 to the STAT1 promoter. Ace also suppressed the Th17 differentiation of $CD4^+$ T cells, which was counteracted by HDAC2 overexpression, while STAT1 overexpression offset the regulatory effect of HDAC2 overexpression.

Conclusions: Ace mitigates DNCB-induced AD by inhibiting HDAC2 to activate STAT1 and block Th17 differentiation, uncovering a novel HDAC2-STAT1-Th17 regulatory axis and providing a promising metabolite-based therapeutic strategy for AD.

Keywords: acetate; 2,4-dinitrochlorobenzene; atopic dermatitis; histone deacetylase 2; signal transducer and activator of transcription 1

Introduction

Atopic dermatitis (AD), commonly termed atopic eczema, is a persistent inflammatory condition of the skin, with recurrence, pruritus, erythema, xerosis, a positive atopy history, and age-specific dermatitis distribution as hallmarks [1]. Its pathogenesis is complex and multifactorial, involving interactions between environmental/genetic factors, the immune system, and the skin. These interactions lead to impaired skin barrier integrity, skin microbiome dysbiosis, and dysregulated innate/adaptive immune responses [2,3]. Thus, clarifying AD mechanisms is essential for developing novel therapeutic strategies.

$CD4^+$ T cells may differentiate into one of the lineages of regulatory T (Treg) cells, as well as T helper cells (Th1, Th2, and Th17) [4]. Treg cells are immunosuppressive cells that attenuate immune responses by reducing the levels of proinflammatory cytokines [5]. In contrast, Th17 cells are a subset of proinflammatory T helper cells that can release many inflammatory cytokines to mediate acute inflammatory responses, and the differentiation and function of Th17 cells are closely associated with the pathogenesis of AD [5–7]. Furthermore, the induction of Th17 cell differentiation exacerbates psoriasis-like inflammation [8]. Therefore, inhibiting Th17 cell differentiation may represent a promising therapeutic strategy for alleviating AD.

Intestinal and skin microbial dysbiosis is associated with immune response dysregulation and the development of skin diseases like AD [9]. A previous study showed that the content of bifidobacteria in the intestinal flora of AD patients is decreased [9], and bifidobacteria are known to produce acetate (Ace) [10]. Short-chain fatty acids (SCFAs) are generated in the gut microbiota via fermentation of proteins, peptides and dietary carbohydrates [11]. SCFAs are involved in regulating immunological function, inflammation and intestinal permeability [12]. Ace is the most abundant SCFA present in the plasma, followed by propionate and butyrate [13]. Reportedly, Ace alleviates inflammation in multiple diseases, including methionine/choline-deficient diet-induced non-alcoholic steatohepatitis, alcohol use disorders, and polycystic ovarian syndrome [14,15].

Additionally, gut-derived Ace improves skin barrier integrity [16], implying its potential role in treating AD. In metabolic inflammation, the gut microbiota-derived Ace and propionate effectively reverse high-fat diet (HFD)-induced imbalances by reducing Th17 cell populations and pro-inflammatory cytokines [17]. However, whether Ace alleviates AD by inhibiting Th17 activation remains to be investigated.

Ace has been identified as a histone deacetylase (HDAC) inhibitor that reduces HDAC activity in T cells [18]. HDAC is known as a group of enzymes removing the acetyl group from the lysine residues of histones, which have a critical role in regulating gene expression, and the inhibition of HDAC2 in the HDAC family can attenuate liver inflammation in acute liver failure [19]. Pharmacological HDAC inhibition also enhances signal transducer and activator of transcription 1 (STAT1) expression [20]. A study suggested that STAT1 participates in AD progression [21], inhibiting STAT1 phosphorylation ameliorates AD-like skin lesions, and STAT1 activation suppresses Th17 differentiation [22]. Using hTFtarget, we predicted that HDAC2 can bind to STAT1, and further speculated that increased Acetate (Ace) secretion by bifidobacteria inhibits T cell HDAC2, activates STAT1, and further alleviates Th17 differentiation in AD. Herein, we investigated the role of Ace in AD via *in vivo* experiments and explored how Ace modulates Th17 differentiation through the HDAC2-STAT1 axis.

Materials and Methods

Animals

45 male BALB/c mice (8 weeks old, 21 ± 1 g; Taiyuan Central Hospital) were included, where 40 mice were subjected to AD modeling, and the remaining 5 mice underwent the isolation of $CD4^+$ T cells. All animals were housed in standard plastic cages with sawdust as bedding material (23 ± 1 ℃, relative humidity of 50–60%, and a 12-h light/dark circadian cycle). Animals were allowed *ad libitum* access to standard laboratory chow and tap water throughout the experimental period. All animal experiments strictly complied with *the Guidelines for the Care and Use of Laboratory Animals* of the China Council on Animal Care and Use, and were approved by the Animal Ethics Committee of Zhejiang Provincial Laboratory Animal Center (Approval No. ZJCLA-IACUC-20020213).

Animal Model Establishment and Administration

After a simple randomization procedure, the 40 mice were allocated to four groups (10/group): control, AD, AD+Ace-Low dose (L) and AD+Ace-High dose (H). The dorsal skin of mice was shaved, and stimulated by 300 µL of 1% 2,4-dinitrochlorobenzene (DNCB) (237329, Sigma-Aldrich, St. Louis, MO, USA) dissolved in acetone (179124, Sigma-Aldrich, St. Louis, MO, USA): olive oil (HY-108749, MCE, Monmouth Junction, NJ, USA) (3:1) on day 0 for AD modeling. From day 7 to day 48, 200 µL of 0.3% DNCB was administered to the ears on alternating days [23]. Mice in the AD, AD+Ace-L and AD+Ace-H groups were treated as described above. Sodium Ace (CH_3COONa, ≥99%, S2889, Sigma-Aldrich, St. Louis, MO, USA) was dissolved in H_2O. Mice in AD+Ace-L and AD+Ace-H groups received pH-adjusted sodium Ace at a low dosage (Ace-L, 250 mg/kg) or a high dosage (Ace-H, 500 mg/kg) via intraperitoneal injection at 6 pm and 6 am the next day of AD construction [24], while those in control and AD groups only received an equal volume of phosphate-buffered saline (PBS, C0221A, Beyotime, Shanghai, China). 4 h later, the macroscopic situation of mice was observed, and the AD degree was evaluated [25]. The measurement of ear thickness was conducted with dial calipers. After acclimation to the recording cage, mouse scratching behavior was evaluated. An assessor blinded to the experimental design manually recorded the total number of scratching bout over 10-minute periods. A scratching bout is defined as one complete sequence of lifting a forepaw from the floor, scratching, and then returning the paw to the floor or directing it toward the mouth. Dermatitis was assessed based on symptoms, including edema, erosion, erythema and scaling, each of which was scored as 0 (no symptom), 1 (mild), 2 (moderate), or 3 (severe) [26]. All animals experienced general inhalation anesthesia using 3% isoflurane (792632, Sigma-Aldrich, St. Louis, MO, USA) and oxygen, and were euthanized by cervical dislocation. Dorsal skin, ear skin and splenic tissues were collected, frozen in liquid nitrogen, and stored at –80 ℃.

Splenocyte Isolation

The splenocytes were isolated from the spleens of mice involved in *in vivo* experiments and healthy mice (n = 5) after euthanasia as described above [27]. In brief, spleens were smashed on a 60-mm cell culture dish with 2 mL of Roswell Park Memorial Institute 1640 medium (RPMI-1640, A4192301, Thermo Fisher, Waltham, MA, USA). The medium was transferred and left for the precipitation of the insoluble cells. After centrifugation (316 ×g, 5 min, 4 ℃), the cell pellet was treated (10 min, room temperature (RT)) with ammonium-chloride-potassium (ACK) lysis buffer (A1049201, Thermo Fisher, Waltham, MA, USA; 1 mL ACK buffer/a spleen). The lysed splenocytes were washed thrice with RPMI-1640 medium, and resuspended in RPMI-1640 medium containing 5% fetal bovine serum (FBS, 12483020, Thermo Fisher, Waltham, MA, USA) and 1% penicillin-streptomycin (30-2300, ATCC, Manassas, VA, USA).

Isolation, Transfection and Treatment of $CD4^+$ T cells

Fully automated cell labeling and separation of $CD4^+$ T cells from the splenocytes of healthy mice was completed

using a CD4$^+$ T Cell Isolation Kit (130-104-454, Miltenyi, Bergisch Gladbach, Germany) and the autoMACS® Pro Separator (130-092-545, Miltenyi, Bergisch Gladbach, Germany). CD4$^+$ T cells (5×10^4 cells/well) were cultured (5 days, 37 ℃, 5% CO_2) in a 96-well plate (CLS3922, Sigma-Aldrich, St. Louis, MO, USA) with anti-CD3 (5 µg/mL, 746368, BD Biosciences, San Jose, CA, USA) and anti-CD28 (5 µg/mL, 752543, BD Biosciences, San Jose, CA, USA) for activation. For cell transfection, Yunzhou Biosciences (Guangzhou) Co., Ltd. provided plasmids overexpressing HDAC2 (pRP[Exp]-EGFP/Puro-CAG>mHdac2[NM_008229.2]) or STAT1 (pRP[Exp]-EGFP/Puro-CAG>mStat1[NM_001205313.1]) and its negative control (NC, pRP[Exp]-CAG>ORF_Stuffer:IRES:EGFP/Puro). Activated CD4$^+$ T cells were transfected with the above plasmids/NC, or co-transfected with plasmids overexpressing HDAC2 and STAT1 at a high density using Lipofectamine™ 3000 (L3000015, Thermo Fisher, Waltham, MA, USA). The skewing condition of Th17 was as follows: 1 ng/mL recombinant mouse transforming growth factor-beta1 (TGF-β1, HY-P7117, MedChemExpress, Monmouth Junction, NJ, USA), 40 ng/mL recombinant mouse interleukin (IL)-6 (rmIL-6, 406-ML, R&D Systems, Minneapolis, MN, USA), 40 ng/mL rmIL-23 (1887-ML, R&D Systems, Minneapolis, MN, USA), 20 µg/mL anti-IL-4 (BE0045, Bio X Cell, West Lebanon, NH, USA), and 20 µg/mL anti-interferongamma (IFNγ) (BE0055, Bio X Cell, West Lebanon, NH, USA). Treg stimulations were supplemented with 5 ng/mL TGF-β1 (C16W, Novoprotein, Suzhou, Jiangsu, China), 20 ng/mL IL-2 (CK24, Novoprotein, Suzhou, Jiangsu, China), 10 µg/mL anti-IL-4, and 10 µg/mL anti-IFNγ [28]. The cells after transfection were treated under a Th17 cell-inducing condition with/without 10 mM Ace (72 h) [24].

Hematoxylin-Eosin (H&E) Staining

Dorsal tissue was fixed in 10% formalin (G2161, Solarbio, Beijing, China), decalcified using 5% nitric acid (438073, Sigma-Aldrich, St. Louis, MO, USA), dehydrated in 70%–95% ethanol (E111991, aladdin, Shanghai, China), transparentized in xylene (X112054, aladdin, Shanghai, China) and embedded in paraffin. Then, 8-µm sections were prepared, followed by deparaffinization and treatment with 95%–70% ethanol. Subsequently, sections were stained with 1 mL hematoxylin (8 min; H8070, Solarbio, Beijing, China), differentiated in 5% acetic acid solution (A291611, aladdin, Shanghai, China) and rinsed in running water. Following treatment with 0.5% Ammonium Hydroxide (A299569, aladdin, Shanghai, China) and washing, sections were dyed with 0.5% eosin (3 min; E292725, aladdin, Shanghai, China). Visualization of pathological changes was conducted employing a light microscope (×40 magnification; WMS-1033, WUMO, Shanghai, China).

Western Blot Analysis

Total protein from skin tissue using a radioimmunoprecipitation assay (RIPA) lysis buffer (P0013C, Beyotime, Shanghai, China) underwent concentration determination exploiting the Pierce™ bicinchoninic acid (BCA) Protein Assay Kit (23225, Thermo Fisher, Waltham, MA, USA). Following protein separation using sodium dodecyl sulphate polyacrylamide gel electrophoresis (SDS-PAGE, P0012A, Beyotime, Shanghai, China) and electrotransferrence to polyvinylidene difluoride (PVDF) membranes (88518, Thermo Fisher, Waltham, MA, USA), blockage of membranes was performed with 5% skim milk (2 h, RT). Next, membranes underwent incubation (4 ℃, overnight) with primary antibodies (Abcam, Cambridge, UK), including HDAC2 (ab32117, 55 kDa, 1:2000), STAT1 (ab92506, 87 kDa, 1:1000) and the inner control glyceraldehyde-3-phosphate dehydrogenase (GAPDH, ab8245, 36 kDa, 1:1000). The blots were subsequently washed with Tris-buffered saline with 0.1% Tween-20 (TBST, T1081, Solarbio, Beijing, China) and incubated with Goat Anti-Rabbit IgG (AP132, 1:3000, Sigma-Aldrich, USA) or Goat Anti-Mouse IgG (AP124, 1:3000, Sigma-Aldrich, USA) (RT, 1 h). Specific proteins were detected using the Chemiluminescent Substrate (34577, Thermo Fisher, Waltham, MA, USA). The signals were captured on the Odyssey® M Imaging System (version 2.1, LI-COR Biosciences, Lincoln, Nebraska, USA), and the intensity of proteins was quantified with ImageJ software (version 1.8.0, National Institutes of Health, Bethesda, Maryland, USA).

Chromatin Immunoprecipitation (ChIP)

The correlation between HDAC2 and STAT1 promoter in AD, AD+Ace-H and control skin tissue, as well as in Th17-polarized CD4$^+$ T cells, was verified using ChIP. Skin tissue was cross-linked (RT, 15 min) with formaldehyde (F111941, aladdin, Shanghai, China) and centrifuged (5 min, 300 ×g, 4 ℃). The precipitant was collected, added with PBS and centrifuged (5 min, 1000 rpm, 4 ℃). The collected cells were resuspended in 1 mL lysis buffer (NUC101, Sigma-Aldrich, St. Louis, MO, USA) supplemented with proteases and phosphatases inhibitors (PPC1010, Sigma-Aldrich, St. Louis, MO, USA) and incubated on ice for 30 min, followed by sonication (20 min) using a Bioruptor bath sonicator (Diagenode, Liège, Belgium) at high power with 30 s on/30 s off pulse cycles. DNA fragments ranging from 200 to1000 bp were obtained. After centrifugation (15 min, 16,000 ×g, 4 ℃), the supernatant was collected and diluted with IP buffer (20-153, Sigma-Aldrich, St. Louis, MO, USA). One aliquot of supernatant served as the input control. Each 500 µL sample was incubated overnight (4 ℃) with 15 µL Protein A/G Magnetic beads (88802, Thermo Fisher, Waltham, MA, USA) pre-conjugated with 2 µg anti-HDAC2 (ab124974, Abcam, Cambridge, UK) or control IgG (3900, CST, Dan-

vers, MA, USA). The sample was washed with Tris-EDTA buffer (93283, Sigma-Aldrich, St. Louis, MO, USA), followed by elution with elution buffer (0.1 M NaHCO3, 1% SDS). Subsequently, DNA–protein cross-links were reversed, and DNA was purified using a DNA Purification Kit (D0033, Beyotime, Shanghai, China) and subjected to qPCR analysis. Primer sequences for STAT1 promoter were 5′-TTGGCTCTCTTATCCTGCCG-3′ and 5′-ACGAGACATCATAGGCAGCG-3′.

Quantitative Reverse Transcription Real Time Polymerase Chain Reaction (qRT-PCR)

Total RNA from mouse skin tissue and $CD4^+$ T cells was isolated using an RNA extraction kit (R1200, Solarbio, Beijing, China). The RNA was quantified using a UV spectrophotometer (DR6000, HACH, Beijing, China) and then converted to complementary DNA (cDNA) with a Primescript™ RT reagent Kit (RR037A, Takara, Shiga, Japan). qRT-PCR was performed with SYBR Premix Ex Taq II (RR820A, Takara, Shiga, Japan) using the StepOne Plus real-time PCR system (4376600, Thermo Fisher, Waltham, MA, USA). The cycling conditions were as follows: 5 min (95 ℃); 10 s (95 ℃), 20 s (60 ℃) and 20 s (72 ℃) for 45 cycles; and 10 min (72 ℃). Gene expression was normalized to GAPDH, and relative fold changes were calculated using the $2^{-\Delta\Delta ct}$ method. Primer sequences were listed below: *IL-4*, forward (F): 5′-CCATATCCACGGATGCGACA-3′, reverse (R): 5′-AAGCCCGAAAGAGTCTCTGC-3′; *IL-13*, F: 5′-TGCCATCTACAGGACCCAGA-3′, R: 5′-CTCATTAGAAGGGGCCGTGG-3′; *IL-33*, F: 5′-TCACTGCAGGAAAGTACAGCAT-3′, R: 5′-TTTGCCGGGGAAATCTTGGA-3′; suppression of tumorigenicity 2 (*ST2*), F: 5′-TGTATTTGACAGTTACGGAGGGC-3′, R: 5′-ACTTCAGACGATCTCTTGAGACA-3′; GATA binding protein 3 (*GATA3*), F: 5′-CTGGCGCCGTCTTGATAGTT-3′, R: 5′-GCTCAGAGACGGTTGCTCTT-3′; *IL-1β*, F: 5′-TGCCACCTTTTGACAGTGATG-3′, R: 5′-AAGGTCCACGGGAAAGACAC-3′; tumor necrosis factor-alpha (*TNF-α*), F: 5′-ACCCTCACACTCACAAACCA-3′, R: 5′-ATAGCAAATCGGCTGACGGT-3′; *IL-17*, F: 5′-CAGCAGCGATCATCCCTCAA-3′, R: 5′-TTTCCCTCCGCATTGACACA-3′; *IL-10*, F: 5′-AGGCGCTGTCATCGATTTCT-3′, R: 5′-GCTCTGTCTAGGTCCTGGAGT-3′; *HDAC2*, F: 5′-GGCGGCAAGAAGAAAGTGTG-3′, R: 5′-CAGAGGCAGTGCACCCTAAA-3′; *STAT1*, F: 5′-TTGGCTCTCTTATCCTGCCG-3′, R: 5′-ACGAGACATCATAGGCAGCG-3′; *GAPDH*, F: 5′-AGGTCGGTGTGAACGGATTTG-3′, R: 5′-GGGGTCGTTGATGGCAACA-3′.

Flow Cytometry Assay

$CD4^+$ T cells from healthy mice were transfected and treated under a Th17 cell-inducing condition with or without 10 mM Ace treatment (72 h). Phorbol 12-Myristate 13-Acetate (PMA, 50 ng/mL, 79346, Sigma-Aldrich, St. Louis, MO, USA) and ionomycin (1 μg/mL, HY-13434, MedChemExpress, Monmouth Junction, NJ, USA) were used to stimulate mouse splenocytes from *in vivo* experiments and $CD4^+$ T cells from healthy mice (4 h, 37 ℃), followed by stimulation with Golgistop (554724, BD Biosciences, San Jose, CA, USA). Subsequently, all cells were subjected to the following staining procedures.

Treg cells in mouse splenocytes were assessed using *in vivo* experiments. The single-cell suspensions were first stained with anti-CD4-FITC (11-0041-82, Thermo Fisher, Waltham, MA, USA) and anti-CD25-phycoerythrin (PE) (12-0259-42, Thermo Fisher, Waltham, MA, USA) (30 min, 4 ℃). $CD4^+$ cells were gated at this step. Following fixation and permeabilization, the $CD4^+$-gated cells were then incubated intracellularly with anti-Forkhead box protein 3 (FoxP3)-FITC (11-4777-42, Thermo Fisher, Waltham, MA, USA) for 30 min at 4 ℃ to identify Treg cells.

Th17 cells were identified in mouse splenocytes and $CD4^+$ T cells. In brief, surface staining was performed using anti-CD4-FITC for 30 min at 4 ℃. Then, intracellular cytokine staining was performed using anti-IL-17A-PE (561020, BD Biosciences, San Jose, CA, USA) (30 min, 4 ℃). The specificity of antibodies was ensured with isotype controls in all staining procedures. Flow cytometry was performed using the Attune NxT flow cytometry (A24860, Thermo Fisher, Waltham, MA, USA) with FlowJo software (version 10.8.2, Becton, Dickinson and Company, Ashland, OR, USA).

Statistical Analysis

All statistical analyses were performed using GraphPad Prism 8.0 (GraphPad Software, San Diego, CA, USA). Data normality was assessed for all datasets. Data that were not normally distributed are presented as the median with interquartile range (IQR; P25, P75), while normally distributed data are expressed as the mean ± standard deviation (SD). Multi-group comparisons were performed using the Kruskal-Wallis H test (non-normally distributed data) or one-way analysis of variance (ANOVA) (normally distributed data), followed by Dunn's test or Tukey's test for posthoc multiple comparisons, respectively. Comparisons between two groups were conducted using the independent samples *t*test. p-values < 0.05 were considered statistically significant.

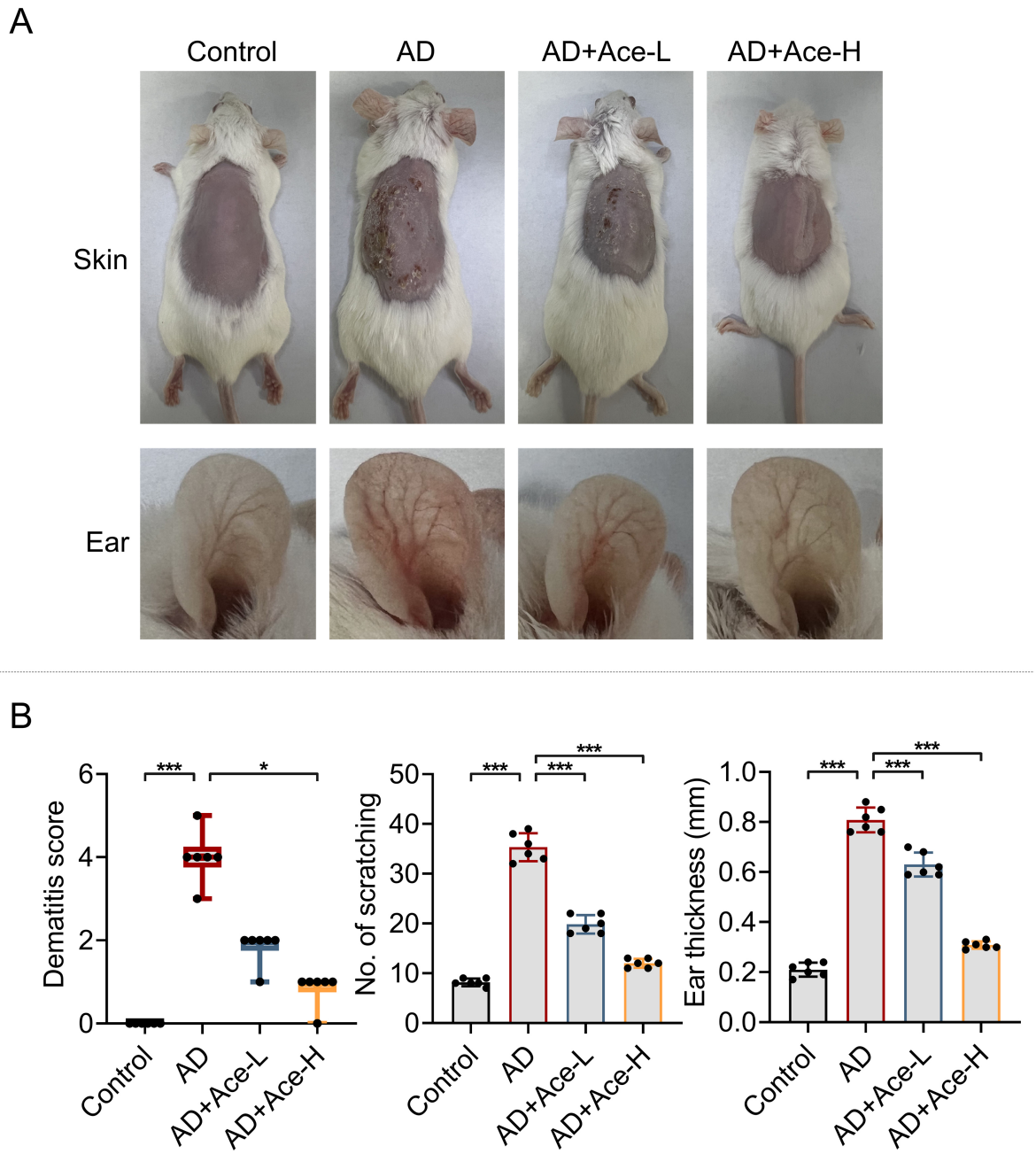

Fig. 1. Ace alleviated AD in a DNCB -induced AD mouse model. (A) The macroscopic situation of mouse skin and ear. (B) The degree of AD in mice (dematitis scores, number of scratching and ear thickness). Data that were not normally distributed are presented as the median with interquartile range (IQR; P25, P75), while normally distributed data are expressed as the mean ± standard deviation (SD). There were six biological replicates in each experimental group (n = 6). $^{*}p < 0.05$, $^{***}p < 0.001$. Groups at both ends of the horizontal lines in the figure were compared. Ace, acetate; AD, atopic dermatitis; DNCB, 2,4-dinitrochlorobenzene; Ace-L, sodium Ace at a low dosage; Ace-H, sodium Ace at a high dosage.

Results

Ace Alleviated AD Symptoms in a DNCB-Induced AD Mouse Model

To observe how Ace affects AD *in vivo*, mice were exposed to 300 µL of 1% DNCB on day 0 and 200 µL of 0.3% DNCB on alternating days for 48 days from day 7. Mice received Ace-L (250 mg/kg) or Ace-H (500 mg/kg) twice via intraperitoneal injection the next day of AD modeling, followed by the observation of the macroscopic situation. We found the dorsal skin of mice in the AD group showed severe dryness, erythema, dandruff and erosion, and the ears became red and swollen following DNCB treatment (Fig. 1A). Interestingly, Ace treatment dose-dependently

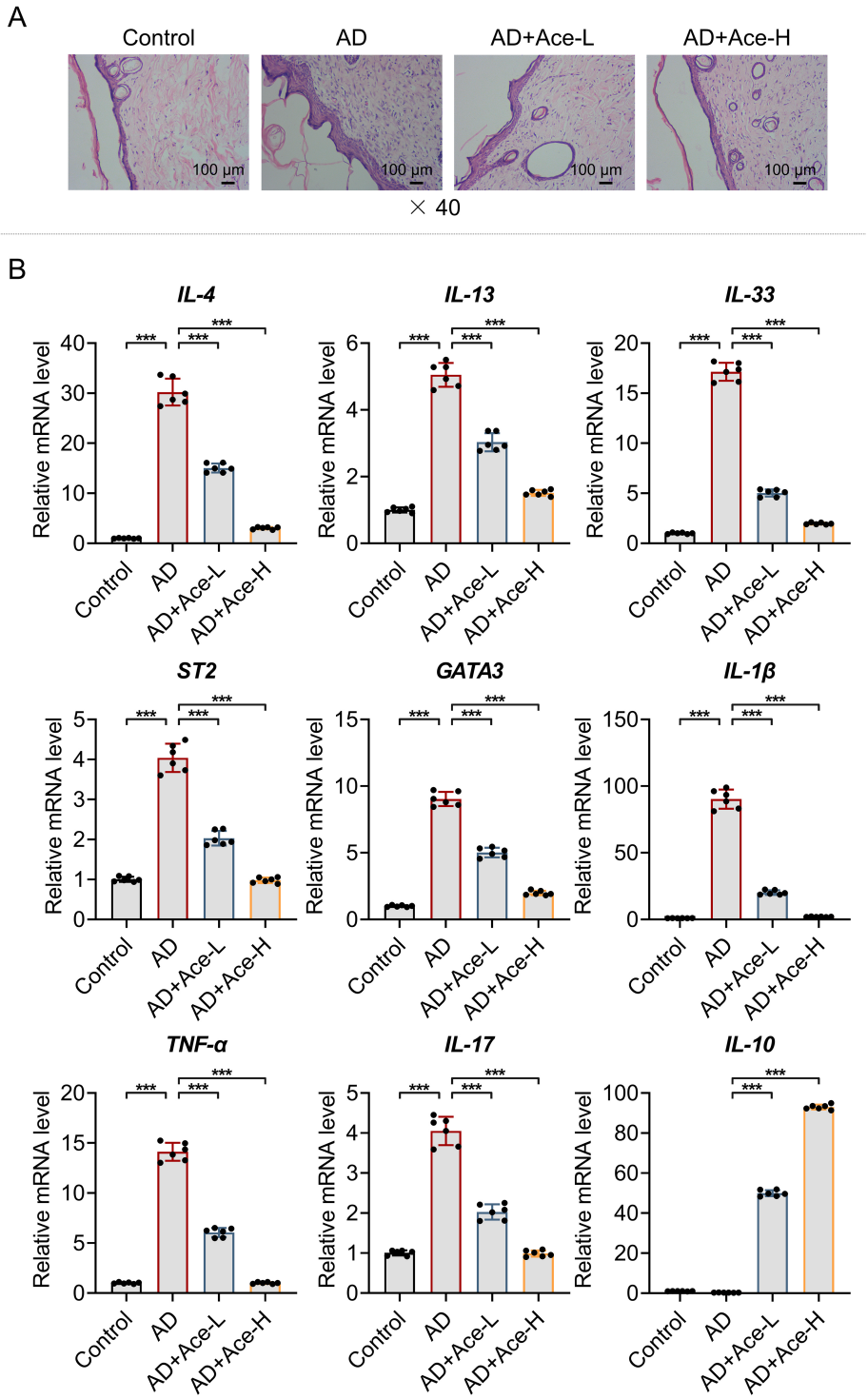

Fig. 2. Ace mitigated DNCB-induced dorsal AD lesions and skin inflammation in mice. (A) The pathological condition of mouse dorsal tissues (H&E staining). Scale bar = 100 μm, magnification, ×40. (B) The expression levels of inflammatory cytokines, including *IL-4*, *IL-13*, *IL-33*, *ST2*, *GATA3*, *IL-1β*, *TNF-α*, *IL-17* and *IL-10* in mouse skin tissues using qRT-PCR. *GAPDH* was used as a loading control. Data are expressed as the mean ± standard deviation (SD). There were three or six biological replicates in each experimental group (n = 3 for A, n = 6 for B). $^{***}p < 0.001$. Groups at both ends of the horizontal lines in the figure were compared. Ace, acetate; DNCB, 2,4-dinitrochlorobenzene; AD, atopic dermatitis; Ace-L, sodium Ace at a low dosage; Ace-H, sodium Ace at a high dosage; H&E, hematoxylin-eosin; IL-4, interleukin-4; ST2, suppression of tumorigenicity 2; GATA3, GATA binding protein 3; TNF-α, tumor necrosis factor-alpha; qRT-PCR, quantitative real time polymerase chain reaction; GAPDH, glyceraldehyde-3-phosphate dehydrogenase.

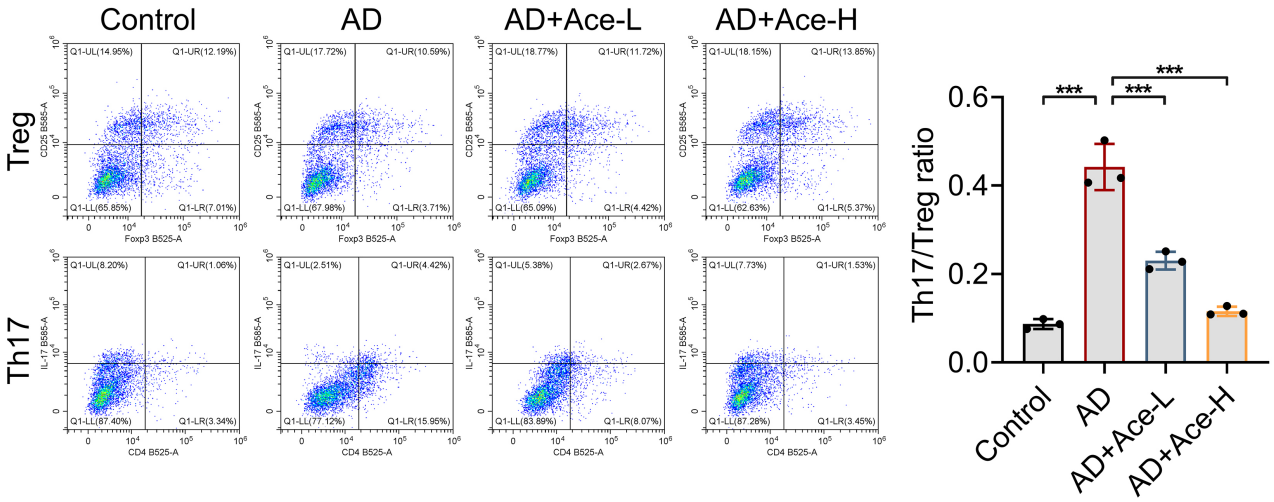

Fig. 3. Ace abrogated DNCB-induced increase of Th17/Treg in mouse splenocytes. Data are expressed as the mean ± standard deviation (SD). There were three biological replicates in each experimental group (n = 3). $^{***}p < 0.001$. Groups at both ends of the horizontal lines in the figure were compared. Ace, acetate; DNCB, 2,4-dinitrochlorobenzene; Th17, T helper 17; Treg, regulatory T; Ace-L, sodium Ace at a low dosage; Ace-H, sodium Ace at a high dosage; AD, atopic dermatitis.

alleviated the skin lesions in AD mice (Fig. 1A). Compared with mice in the control group, mice after AD modeling had higher dematitis scores, increased scratching frequency and greater ear thickness (Fig. 1B, $p < 0.05$). Ace-H decreased dematitis score in model mice (Fig. 1B, $p < 0.05$), while both Ace-L and Ace-H significantly reduced the scratching frequency and ear thickness (Fig. 1B, $p < 0.05$). Thus, Ace may play a therapeutic role in a DNCB-induced AD mouse model.

Ace Mitigated DNCB-Induced Dorsal AD Lesions and Skin Inflammation in Mice

According to H&E staining data, DNCB-induced mice presented the typical microscopic characteristics of dermatitis, including thickened epidermal and dermal tissues and inflammatory cell infiltration (Fig. 2A). However, Ace treatment, especially Ace-H, restored epidermal and dermal thickness and decreased cell infiltration in model mice (Fig. 2A). The inflammatory cytokines, including *IL-4*, *IL-13*, *IL-33*, *ST2*, *GATA3*, *IL-1β*, *TNF-α* and *IL-17*, were up-regulated in skin tissue from the AD mice (Fig. 2B, $p < 0.05$), while IL-10 showed a downward trend (without statistical significance) (Fig. 2B). Both Ace-L and Ace-H could reverse the above trends of inflammatory cytokines in AD mice (Fig. 2B, $p < 0.05$). Consequently, Ace mitigated DNCB-induced dorsal AD lesions and skin inflammation in mice.

Ace Abrogated DNCB-Induced Increase of Th17/Treg in Mouse Splenocytes

Then, flow cytometry was performed to assess the Th17/Treg ratio in mouse splenocytes. The results exhibited that the ratio was increased in splenocytes of mice after modeling (Fig. 3, $p < 0.05$), while the increase was offset upon treatment with Ace-L or Ace-H (Fig. 3, $p < 0.05$).

Ace Reversed DNCB-Induced Up-Regulation of HDAC2 and Down-Regulation of STAT1, and HDAC2 Bound to the STAT1 Promoter in Mouse Skin Tissues

The DNCB-induced AD mouse model presented higher HDAC2 levels and lower STAT1 levels in skin tissue (Fig. 4A, $p < 0.05$), while both Ace-L (Fig. 4A, $p < 0.05$) and Ace-H (Fig. 4A, $p < 0.05$) treatment significantly down-regulated HDAC2 and up-regulated STAT1 in the skin tissue from model mice. ChIP analysis data verified that Ace treatment effectively reduced HDAC2 enrichment at the STAT1 promoter. This effect was observed both in skin tissue and in control $CD4^+$ T cells cultured in Th17-polarizing medium (Fig. 4B,C, $p < 0.05$).

HDAC2 Overexpression Offset Ace-Inhibited Th17 Differentiation in $CD4^+$ T Cells by Down-Regulating STAT1

Transfection with plasmids overexpressing HDAC2 or STAT1 evidently up-regulated HDAC2 (Fig. 5A, $p < 0.05$) or STAT1 (Fig. 5B, $p < 0.05$) in $CD4^+$ T cells respectively, indicating successful transfection. To explore how HDAC2, Ace and STAT1 affect Th17 differentiation of $CD4^+$ T cells, the transfected cells were treated under a Th17 cell-inducing condition with or without 10 mM Ace for 72 h. The results of flow cytometry showed Ace suppressed Th17 differentiation of $CD4^+$ T cells (Fig. 5C, $p < 0.05$). This inhibitory effect was partially counteracted by HDAC2 overexpression (Fig. 5C, $p < 0.05$) but further enhanced by STAT1 overexpression (Fig. 5C, $p <$

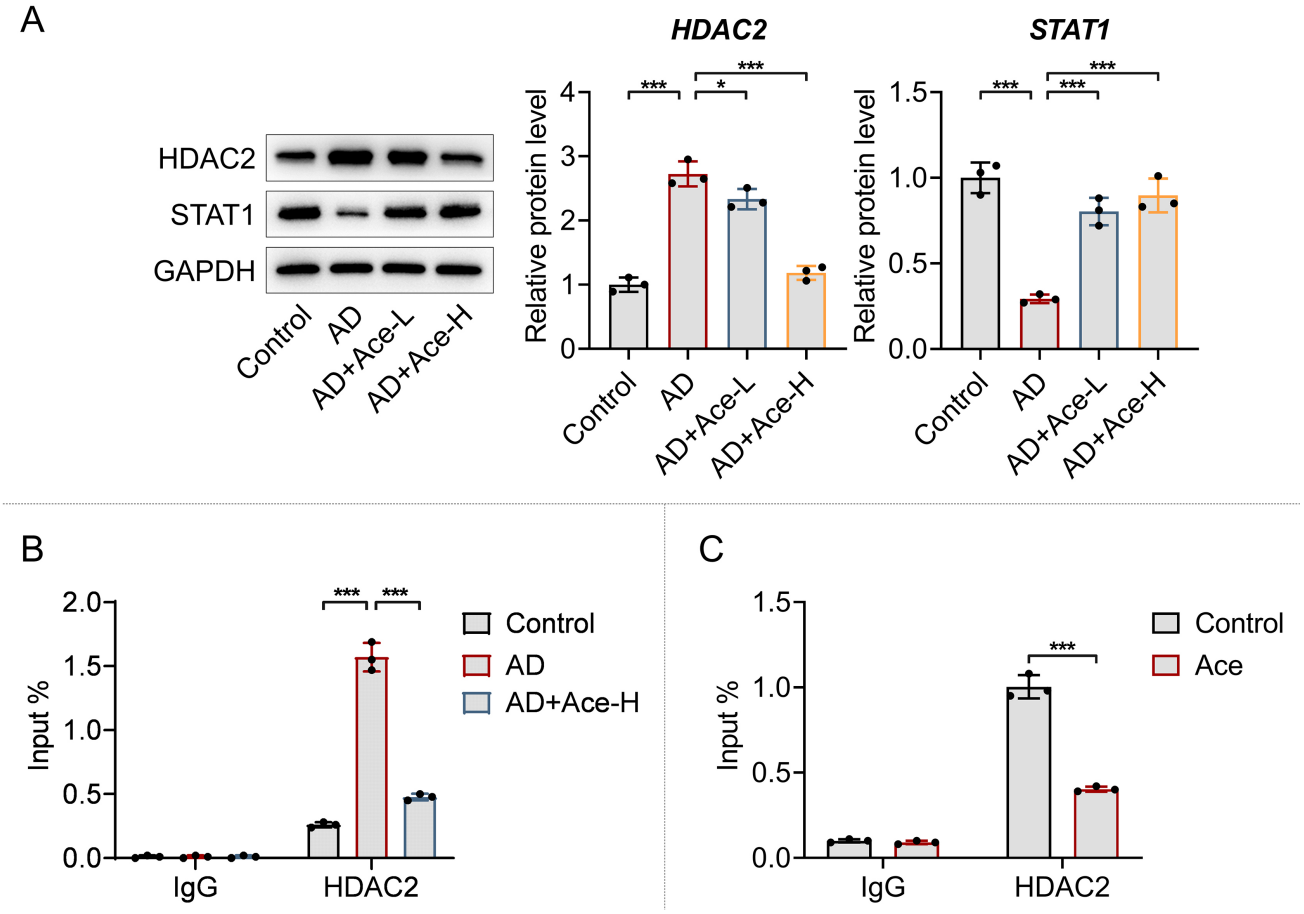

Fig. 4. Ace reversed DNCB-induced up-regulation of HDAC2 and down-regulation of STAT1, and HDAC2 bound to STAT1 promoter in mouse skin tissues. (A) HDAC2 and STAT1 expression levels in mouse skin tissues using Western blotting. GAPDH was used as a loading control. (B) The correlation between HDAC2 and the STAT1 promoter in mouse skin tissue using ChIP. (C) The correlation between HDAC2 and the STAT1 promoter in $CD4^+$ T cells using ChIP. (Control: Th17-polarized $CD4^+$ T cells). Data are expressed as the mean ± standard deviation (SD). There were three biological replicates in each experimental group (n = 3). $^*p < 0.05$, $^{***}p < 0.001$. Groups at both ends of the horizontal lines in the figure were compared. Ace, acetate; DNCB, 2,4-dinitrochlorobenzene; HDAC2, histone deacetylase 2; STAT1, signal transducer and activator of transcription 1; Ace-L, sodium Ace at a low dosage; Ace-H, sodium Ace at a high dosage; AD, atopic dermatitis; GAPDH, glyceraldehyde-3-phosphate dehydrogenase; ChIP, chromatin immunoprecipitation.

0.05), denoting that HDAC2 and STAT1 exert opposite effects in Ace-regulated Th17 differentiation, and that STAT1 overexpression can partially offset the recovery effect of HDAC2 overexpression.

Discussion

AD has an increasing incidence with the development of urbanization and industrialization, which affects 10% of adults and 15–30% of children and brings a great economic burden to patients worldwide [29–31]. Therefore, exploring novel therapeutic strategies for AD is of great importance. BALB/c mice were topically treated with DNCB to induce AD-like skin lesions in our *in vivo* study [32]. We found DNCB induced AD symptoms, dorsal AD lesions and up-regulation of proinflammatory factors in skin tissue in mice.

Current research suggested that intestinal microorganisms can affect other organs, and the gut and skin have intimate associations with changes in immune response and AD development [9]. The content of bifidobacteria is reduced in the intestinal flora in AD patients, and bifidobacteria can produce Ace [9,10]. Ace has demonstrated anti-inflammatory action in various models [14,33,34]. More importantly, the association between lower acetate levels in the breast milk and AD in infancy has been confirmed [35]. Furthermore, Ace derived from the gut improves skin barrier integrity via enhancing keratinocyte metabolism and differentiation, which may limit allergen sensitization and AD development [16]. However, the exact functions of Ace in the pathogenic processes of AD are poorly defined.

Herein, Ace mitigated DNCB-induced AD symptoms and dorsal AD lesions in mice, as evidenced by down-regulation of *IL-4*, *IL-13*, *IL-33*, *ST2*, *GATA3*, *IL-1β*, *TNF-*

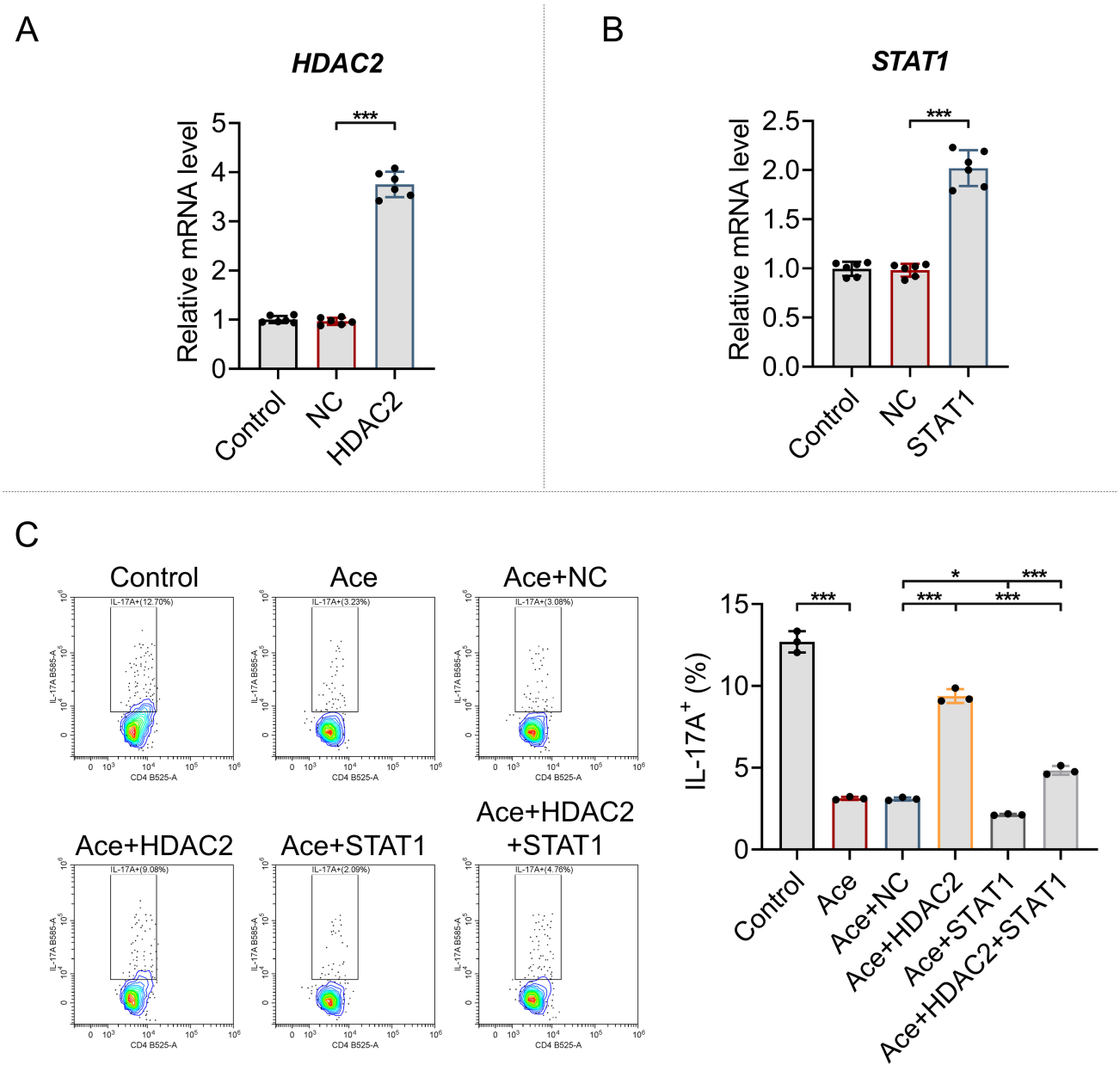

Fig. 5. HDAC2 overexpression offset Ace-inhibited Th17 differentiation in CD4$^+$ T cells by down-regulating STAT1. (A) *HDAC2* expression in CD4$^+$ T cells after transfection with plasmids overexpressing HDAC2 using qRT-PCR. *GAPDH* was used as a reference gene. (B) *STAT1* expression in CD4$^+$ T cells after transfection with plasmids overexpressing STAT1 was identified using qRT-PCR. *GAPDH* was used as a reference gene. (C) Th17 differentiation in CD4$^+$ T cells transfected with plasmids overexpressing HDAC2/STAT1 or NC and treated under a Th17 cell-inducing condition with or without 10 mM Ace for 72 h (flow cytometry). Data are expressed as the mean ± standard deviation (SD). There were three or six biological replicates in each experimental group (n = 6 for A, B, n = 3 for C). $^*p < 0.05$, $^{***}p < 0.001$. Groups at both ends of the horizontal lines in the figure were compared. HDAC2, histone deacetylase 2; Ace, acetate; Th17, T helper 17; STAT1, signal transducer and activator of transcription 1; qRT-PCR, quantitative real time polymerase chain reaction; GAPDH, glyceraldehyde-3-phosphate dehydrogenase; NC, negative control.

α and *IL-17* levels, as well as up-regulation of IL-10 levels in the skin tissues of AD mice. Th17 cells are proinflammatory T helper cells producing IL-17, inducing the production of inflammatory cytokines [7]. Th17 activation and Th17/Treg imbalance can result in prolonged inflammation [36]. Additionally, Th17/Treg imbalance can contribute to the pathogenesis and development of AD [37]. Herein, Ace alleviated DNCB-induced increase of Th17/Treg in mouse splenocytes, suggesting that Ace plays a therapeutic role in DNCB-induced AD.

Ace can suppress HDAC and decrease the activity of HDAC in T cells [18,38]. HDAC6 mediates AD via reg-

ulating cellular interactions and expression levels of microRNA (miR)-9 and sirtuin 1 (SIRT1) [39]. HDAC2 is a class I histone deacetylase implicated in mediating different cellular processes, including cell apoptosis, development, differentiation, proliferation, senescence, cycle and glucocorticoid function in inflammatory reactions [40]. Feng *et al*. [41] reported that HDAC2 inhibitors suppress respiratory syncytial virus (RSV) infection and relieve virus-induced airway inflammation. Jiao *et al*. [42] confirmed that HDAC2 inhibitor CAY10683 reduces lipopolysaccharide-induced neuroinflammation by attenuating Toll-like Receptor 4 (TLR4)/NF-κB signaling pathway. Nonetheless, the specific contribution of HDAC2 in Ace-mediated amelioration of AD remained unclear. Herein, we identified HDAC2 as a key target, overexpression of which reversed the inhibitory effect of Ace on Th17 differentiation in $CD4^+$ T cells.

Beyond confirming Ace as an HDAC inhibitor, this study further elucidated its downstream mechanism. As a previous study indicated, pharmacological inhibition of HDAC activity promotes STAT1 expression [20]. hTF-target predicted that HDAC2 can bind to STAT1, which is consistent with our results. STAT1 is involved in AD development [21]. In addition, STAT1 activation suppresses Th17 differentiation [43]. Impressic acid ameliorates AD-like skin lesions by inhibiting extracellular signal-regulated protein kinase (ERK1/2)-mediated phosphorylation of NF-κB and STAT1 [22]. Nevertheless, the mechanism by which Ace modulates AD via Th17 differentiation through the HDAC2/STAT1 pathway remains poorly understood. In this study, we demonstrated that HDAC2 can bind to STAT1. Functionally, STAT1 overexpression enhanced, whereas HDAC2 overexpression attenuated the suppressive effect of Ace on Th17 differentiation, indicating the HDAC2/STAT1 axis as a central pathway through which Ace exerts its function. While previous studies established Ace as an HDAC inhibitor and separately established STAT1 as a regulator of Th17 differentiation, our study integrated these findings by providing direct experimental evidence that Ace inhibits HDAC2 to modulate STAT1 activity, thereby restraining Th17 differentiation. This represents a novel mechanistic insight into how a gut-derived metabolite can epigenetically regulate T-cell polarization to alleviate AD. Although AD is primarily driven by a Th2-type immune response, our findings suggest that acetate's modulation of the Th17/Treg axis may interact with Th2-mediated pathways. Emerging evidence indicates that Th17 and Th2 responses can synergize to exacerbate skin inflammation in AD [44]. Therefore, the regulation of Th17 cells by acetate may not only address a specific inflammatory arm but also indirectly influence the broader Th2-dominated disease context, highlighting its potential as a multi-faceted immunomodulator.

In this study, Ace was administered via intraperitoneal injection to validate its systemic immunomodulatory function. While this peripheral route differs from the endogenous physiological pathway where microbial-derived Ace is absorbed via the portal vein, it effectively models systemic exposure and provides direct mechanistic evidence for the potential role of gut-derived Ace in the gut-skin axis. Future studies measuring intestinally derived Ace are warranted to validate its physiological transport and function.

However, this study has several limitations. First, it relied solely on mouse models and *in vitro* cell experiments, lacking clinical data from human subjects to validate the findings. Second, detection of anti-inflammatory factor was insufficient, as only *IL-10* levels in skin tissue were assessed, while AD's inflammatory balance involves multiple anti-inflammatory mediators (e.g., *TGF-β*, *IL-35*). Future research should explore Ace's effects in human trials and further investigate additional underlying mechanisms.

Conclusions

In summary, Ace alleviates DNCB-induced AD by suppressing HDAC2 expression, thereby activating STAT1 and inhibiting Th17 differentiation, which indicates its potential anti-AD effects.

Availability of Data and Materials

The analyzed data sets generated during the study are available from the corresponding author on reasonable request.

Author Contributions

XH and XL designed the research study. HF performed the research. HF collected and analyzed the data. XH has been involved in drafting the manuscript and all authors have been involved in revising it critically for important intellectual content. All authors gave final approval of the version to be published. All authors have participated sufficiently in the work to take public responsibility for appropriate portions of the content and agreed to be accountable for all aspects of the work in ensuring that questions related to its accuracy or integrity.

Ethics Approval and Consent to Participate

All animal experiments were performed in strict compliance with the *Guidelines for the Care and Use of Laboratory Animals* of the China Council on Animal Care and Use, and were approved by the Animal Ethics Committee of Zhejiang Provincial Laboratory Animal Center (Approval No. ZJCLA-IACUC-20020213).

Acknowledgment

Not applicable.

Funding

This research received no external funding.

Conflict of Interest

The authors declare no conflict of interest.

References

[1] Alsabbagh M, Ismaeel A. The role of cytokines in atopic dermatitis: a breakthrough in immunopathogenesis and treatment. Acta Dermatovenerologica Alpina, Pannonica, et Adriatica. 2022; 31: 13–31.

[2] Weidinger S, Beck LA, Bieber T, Kabashima K, Irvine AD. Atopic dermatitis. Nature Reviews. Disease Primers. 2018; 4: 1. https://doi.org/10.1038/s41572-018-0001-z.

[3] Eyerich K, Eyerich S, Biedermann T. The Multi-Modal Immune Pathogenesis of Atopic Eczema. Trends in Immunology. 2015; 36: 788–801. https://doi.org/10.1016/j.it.2015.10.006.

[4] Zhang S, Gang X, Yang S, Cui M, Sun L, Li Z, *et al*. The Alterations in and the Role of the Th17/Treg Balance in Metabolic Diseases. Frontiers in Immunology. 2021; 12: 678355. https://doi.org/10.3389/fimmu.2021.678355.

[5] Bittner S, Hehlgans T, Feuerer M. Engineered Treg cells as putative therapeutics against inflammatory diseases and beyond. Trends in Immunology. 2023; 44: 468–483. https://doi.org/10.1016/j.it.2023.04.005.

[6] Ma L, Xue HB, Wang F, Shu CM, Zhang JH. MicroRNA-155 may be involved in the pathogenesis of atopic dermatitis by modulating the differentiation and function of T helper type 17 (Th17) cells. Clinical and Experimental Immunology. 2015; 181: 142–149. https://doi.org/10.1111/cei.12624.

[7] Jiao A, Yang Z, Fu X, Hua X. Phloretin Modulates Human Th17/Treg Cell Differentiation In Vitro via AMPK Signaling. BioMed Research International. 2020; 2020: 6267924. https://doi.org/10.1155/2020/6267924.

[8] Wu R, Zeng J, Yuan J, Deng X, Huang Y, Chen L, *et al*. MicroRNA-210 overexpression promotes psoriasis-like inflammation by inducing Th1 and Th17 cell differentiation. The Journal of Clinical Investigation. 2018; 128: 2551–2568. https://doi.org/10.1172/JCI97426.

[9] Lee SY, Lee E, Park YM, Hong SJ. Microbiome in the Gut-Skin Axis in Atopic Dermatitis. Allergy, Asthma & Immunology Research. 2018; 10: 354–362. https://doi.org/10.4168/aair.2018.10.4.354.

[10] Fukuda S, Toh H, Hase K, Oshima K, Nakanishi Y, Yoshimura K, *et al*. Bifidobacteria can protect from enteropathogenic infection through production of acetate. Nature. 2011; 469: 543–547. https://doi.org/10.1038/nature09646.

[11] Al-Roub A, Akhter N, Al-Sayyar A, Wilson A, Thomas R, Kochumon S, *et al*. Short Chain Fatty Acid Acetate Increases TNFα-Induced MCP-1 Production in Monocytic Cells via ACSL1/MAPK/NF-κB Axis. International Journal of Molecular Sciences. 2021; 22: 7683. https://doi.org/10.3390/ijms22147683.

[12] Murugesan S, Nirmalkar K, Hoyo-Vadillo C, García-Espitia M, Ramírez-Sánchez D, García-Mena J. Gut microbiome production of short-chain fatty acids and obesity in children. European Journal of Clinical Microbiology & Infectious Diseases. 2018; 37: 621–625. https://doi.org/10.1007/s10096-017-3143-0.

[13] Kwon Y, Cho KH, Ma S, Ko H, Hong GH, Lee SY, *et al*. Supplementation of Heat-Treated *Lactiplantibacillus plantarum* nF1 Changes the Production of Short-Chain Fatty Acids in Healthy Infants. Journal of Nutrition and Metabolism. 2024; 2024: 5558566. https://doi.org/10.1155/2024/5558566.

[14] Olaniyi KS, Areloegbe SE. Suppression of PCSK9/NF-kB-dependent pathways by acetate ameliorates cardiac inflammation in a rat model of polycystic ovarian syndrome. Life Sciences. 2022; 300: 120560. https://doi.org/10.1016/j.lfs.2022.120560.

[15] Deng M, Qu F, Chen L, Liu C, Zhang M, Ren F, *et al*. SCFAs alleviated steatosis and inflammation in mice with NASH induced by MCD. The Journal of Endocrinology. 2020; 245: 425–437. https://doi.org/10.1530/JOE-20-0018.

[16] Trompette A, Pernot J, Perdijk O, Alqahtani RAA, Domingo JS, Camacho-Muñoz D, *et al*. Gut-derived short-chain fatty acids modulate skin barrier integrity by promoting keratinocyte metabolism and differentiation. Mucosal Immunology. 2022; 15: 908–926. https://doi.org/10.1038/s41385-022-00524-9.

[17] Mandaliya DK, Patel S, Seshadri S. The Combinatorial Effect of Acetate and Propionate on High-Fat Diet Induced Diabetic Inflammation or Metaflammation and T Cell Polarization. Inflammation. 2021; 44: 68–79. https://doi.org/10.1007/s10753-020-01309-7.

[18] Olaniyi KS, Amusa OA, Ajadi IO, Alabi BY, Agunbiade TB, Ajadi MB. Repression of HDAC5 by acetate restores hypothalamic-pituitary-ovarian function in type 2 diabetes mellitus. Reproductive Toxicology. 2021; 106: 69–81. https://doi.org/10.1016/j.reprotox.2021.10.008.

[19] Wang Y, Chen Q, Jiao F, Shi C, Pei M, Wang L, *et al*. Histone deacetylase 2 regulates ULK1 mediated pyroptosis during acute liver failure by the K68 acetylation site. Cell Death & Disease. 2021; 12: 55. https://doi.org/10.1038/s41419-020-03317-9.

[20] Kumar P, Gogulamudi VR, Periasamy R, Raghavaraju G, Subramanian U, Pandey KN. Inhibition of HDAC enhances STAT acetylation, blocks NF-κB, and suppresses the renal inflammation and fibrosis in *Npr1* haplotype male mice. American Journal of Physiology. Renal Physiology. 2017; 313: F781–F795. https://doi.org/10.1152/ajprenal.00166.2017.

[21] Kim HJ, Song HK, Park SH, Jang S, Park KS, Song KH, *et al*. Terminalia chebula Retz. extract ameliorates the symptoms of atopic dermatitis by regulating anti-inflammatory factors in vivo and suppressing STAT1/3 and NF-κB signaling in vitro. Phytomedicine. 2022; 104: 154318. https://doi.org/10.1016/j.phymed.2022.154318.

[22] Choi JH, Lee GH, Jin SW, Kim JY, Hwang YP, Han EH, *et al*. Impressic Acid Ameliorates Atopic Dermatitis-Like Skin Lesions by Inhibiting ERK1/2-Mediated Phosphorylation of NF-κB and STAT1. International Journal of Molecular Sciences. 2021; 22: 2334. https://doi.org/10.3390/ijms22052334.

[23] Kang J, Im DS. FFA2 Activation Ameliorates 2,4-Dinitrochlorobenzene-Induced Atopic Dermatitis in Mice. Biomolecules & Therapeutics. 2020; 28: 267–271. https://doi.org/10.4062/biomolther.2019.160.

[24] Daïen CI, Tan J, Audo R, Mielle J, Quek LE, Krycer JR, *et al*. Gut-derived acetate promotes B10 cells with antiinflammatory effects. JCI Insight. 2021; 6: e144156. https://doi.org/10.1172/jci.insight.144156.

[25] Zheng T, Fan M, Wei Y, Feng J, Zhou P, Sun X, *et al*. Huangbai Liniment Ameliorates Skin Inflammation in Atopic Dermatitis. Frontiers in Pharmacology. 2021; 12: 726035. https://doi.org/10.3389/fphar.2021.726035.

[26] Matsuda H, Watanabe N, Geba GP, Sperl J, Tsudzuki M, Hiroi J, *et al*. Development of atopic dermatitis-like skin lesion with IgE hyperproduction in NC/Nga mice. International Immunology. 1997; 9: 461–466. https://doi.org/10.1093/intimm/9.3.461.

[27] Yang EJ, Song KS. The ameliorative effects of capsidiol isolated from elicited Capsicum annuum on mouse splenocyte immune responses and neuroinflammation. Phytotherapy Research. 2021; 35: 1597–1608. https://doi.org/10.1002/ptr.6927.

[28] Du HX, Yue SY, Niu D, Liu C, Zhang LG, Chen J, *et al*. Gut Microflora Modulates Th17/Treg Cell Differentiation in Experimental Autoimmune Prostatitis *via* the Short-Chain Fatty Acid Propionate. Frontiers in Immunology. 2022; 13: 915218. https://doi.org/10.3389/fimmu.2022.915218.

[29] Hidaka T, Ogawa E, Kobayashi EH, Suzuki T, Funayama R, Nagashima T, *et al*. The aryl hydrocarbon receptor AhR links atopic dermatitis and air pollution via induction of the neurotrophic factor artemin. Nature Immunology. 2017; 18: 64–73. https://doi.org/10.1038/ni.3614.

[30] Langan SM, Irvine AD, Weidinger S. Atopic dermatitis. Lancet. 2020; 396: 345–360. https://doi.org/10.1016/S0140-6736(20)31286-1.

[31] Drucker AM, Wang AR, Li WQ, Sevetson E, Block JK, Qureshi AA. The Burden of Atopic Dermatitis: Summary of a Report for the National Eczema Association. The Journal of Investigative Dermatology. 2017; 137: 26–30. https://doi.org/10.1016/j.jid.2016.07.012.

[32] Kim YJ, Choi MJ, Bak DH, Lee BC, Ko EJ, Ahn GR, *et al*. Topical administration of EGF suppresses immune response and protects skin barrier in DNCB-induced atopic dermatitis in NC/Nga mice. Scientific Reports. 2018; 8: 11895. https://doi.org/10.1038/s41598-018-30404-x.

[33] Li M, Hu FC, Qiao F, Du ZY, Zhang ML. Sodium acetate alleviated high-carbohydrate induced intestinal inflammation by suppressing MAPK and NF-κB signaling pathways in Nile tilapia (Oreochromis niloticus). Fish & Shellfish Immunology. 2020; 98: 758–765. https://doi.org/10.1016/j.fsi.2019.11.024.

[34] Xu M, Wang C, Li N, Wang J, Zhang Y, Deng X. Intraperitoneal Injection of Acetate Protects Mice Against Lipopolysaccharide (LPS) Induced Acute Lung Injury Through Its Anti-Inflammatory and Anti-Oxidative Ability. Medical Science Monitor. 2019; 25: 2278–2288. https://doi.org/10.12659/MSM.911444.

[35] Wang LC, Huang YM, Lu C, Chiang BL, Shen YR, Huang HY, *et al*. Lower caprylate and acetate levels in the breast milk is associated with atopic dermatitis in infancy. Pediatric Allergy and Immunology. 2022; 33: e13744. https://doi.org/10.1111/pai.13744.

[36] Yuan M, Qian X, Huang Y, Ma X, Duan F, Yang Y, *et al*. Th17 Activation and Th17/Treg Imbalance in Prolonged Anterior Intraocular Inflammation after Ocular Alkali Burn. International Journal of Molecular Sciences. 2022; 23: 7075. https://doi.org/10.3390/ijms23137075.

[37] Ma L, Xue HB, Guan XH, Shu CM, Wang F, Zhang JH, *et al*. The Imbalance of Th17 cells and CD4(+) CD25(high) Foxp3(+) Treg cells in patients with atopic dermatitis. Journal of the European Academy of Dermatology and Venereology. 2014; 28: 1079–1086. https://doi.org/10.1111/jdv.12288.

[38] Olaniyi KS, Amusa OA, Areola ED, Olatunji LA. Suppression of HDAC by sodium acetate rectifies cardiac metabolic disturbance in streptozotocin-nicotinamide-induced diabetic rats. Experimental Biology and Medicine. 2020; 245: 667–676. https://doi.org/10.1177/1535370220913847.

[39] Kwon Y, Choi Y, Kim M, Jeong MS, Jung HS, Jeoung D. HDAC6 and CXCL13 Mediate Atopic Dermatitis by Regulating Cellular Interactions and Expression Levels of miR-9 and SIRT1. Frontiers in Pharmacology. 2021; 12: 691279. https://doi.org/10.3389/fphar.2021.691279.

[40] Yao H, Rahman I. Role of histone deacetylase 2 in epigenetics and cellular senescence: implications in lung inflammaging and COPD. American Journal of Physiology. Lung Cellular and Molecular Physiology. 2012; 303: L557–L566. https://doi.org/10.1152/ajplung.00175.2012.

[41] Feng Q, Su Z, Song S, Xu H, Zhang B, Yi L, *et al*. Histone deacetylase inhibitors suppress RSV infection and alleviate virus-induced airway inflammation. International Journal of Molecular Medicine. 2016; 38: 812–822. https://doi.org/10.3892/ijmm.2016.2691.

[42] Jiao FZ, Wang Y, Zhang HY, Zhang WB, Wang LW, Gong ZJ. Histone Deacetylase 2 Inhibitor CAY10683 Alleviates Lipopolysaccharide Induced Neuroinflammation Through Attenuating TLR4/NF-κB Signaling Pathway. Neurochemical Research. 2018; 43: 1161–1170. https://doi.org/10.1007/s11064-018-2532-9.

[43] Jia L, Jiang Y, Wu L, Fu J, Du J, Luo Z, *et al*. Porphyromonas gingivalis aggravates colitis via a gut microbiota-linoleic acid metabolism-Th17/Treg cell balance axis. Nature Communications. 2024; 15: 1617. https://doi.org/10.1038/s41467-024-45473-y.

[44] Go HN, Lee SH, Cho HJ, Ahn JR, Kang MJ, Lee SY, *et al*. Effects of chloromethylisothiazolinone/methylisothiazolinone (CMIT/MIT) on Th2/Th17-related immune modulation in an atopic dermatitis mouse model. Scientific Reports. 2020; 10: 4099. https://doi.org/10.1038/s41598-020-60966-8.